Pattern Recognition Using Invariants Defined from Higher Order Spectra—One-Dimensional Inputs

Vinod Chandran, *Member, IEEE*, and Stephen L. Elgar, *Member, IEEE*

***Abstract*—A new approach to pattern recognition using invariant parameters based on higher order spectra is presented. In particular, invariant parameters derived from the bispectrum are used to classify one-dimensional shapes. The bispectrum, which is translation invariant, is integrated along straight lines passing through the origin in bifrequency space. The phase of the integrated bispectrum is shown to be scale and amplification invariant, as well. A minimal set of these invariants is selected as the feature vector for pattern classification, and a minimum distance classifier using a statistical distance measure is used to classify test patterns. The classification technique is shown to distinguish two similar, but different bolts given their one-dimensional profiles. Pattern recognition using higher order spectral invariants is fast, suited for parallel implementation, and has high immunity to additive Gaussian noise. Simulation results show very high classification accuracy, even for low signal-to-noise ratios.**

I. Introduction

THIS paper presents an approach to pattern recognition that utilizes information in the higher order spectrum (or, equivalently, higher order correlations) [1]–[12] of a signal. The use of higher order spectra for feature extraction is motivated by the following observations.

1) Information about the shape of a signal resides primarily in the phase [13] and not in the amplitude of its Fourier transform.

2) Higher order spectra retain both amplitude and phase information from the Fourier transform of the signal, unlike the power spectrum.

3) Higher order spectra are translation invariant and functions can be defined from higher order spectra, as shown here for one-dimensional inputs, that satisfy other desirable properties, such as scaling and amplification invariance. These functions can then serve as invariant features for pattern recognition.

4) Higher order spectra, of order greater than two, have zero expected value for Gaussian noise. Therefore, features derived from them will have high immunity to additive Gaussian noise when higher order spectra from multiple realizations of the signal are averaged [2], [5], [6], [37]. Further, they will be robust to additive Gaussian noise, even for single realizations, if the feature extraction procedure integrates in the higher order spectral domain, as demonstrated below.

The various techniques used for pattern recognition [14]–[30] may be subdivided into two groups: a) those that derive local features which depend only on parts of the object or pattern, and b) those that derive global features or features that depend on the entire object or pattern. The local-feature based methods [14] work well when objects are in a cluttered environment, but local features cannot be extracted from inputs with poor signal-to-noise ratios. Also, several local features are required for accurate classification and the tree of possible correspondences between data features and model features is large, and a search of this tree is often computationally expensive. Global-feature based methods [19]–[30], such as the moment invariant method [22]–[25], usually work with small dimensional feature vectors and can be made to satisfy desirable invariance properties, but their feature extraction procedure is computationally intensive and their performance is poor for low SNR inputs. In this study, a computationally efficient global-feature based pattern recognition method which works well at low signal-to-noise ratios is presented. The features for this method are derived from the bispectrum of the signal. Higher order spectral or higher order correlation-based techniques [31]–[37] have been employed for signal detection and object identification. Some of these techniques [37] employ the sample bicoherence as a detection statistic while others [34], [36] use matched filtering in the cumulant domain. Triple-correlation based classifiers that employ a bank of matched filters [34], [36] are computationally intensive when there are a large number of classes because there must be one filter matched to each class. Moreover, the filters must be normalized to have equal cumulant energies, adding to the complexity of the training process. The technique presented here does not make use of matched filters. It derives features directly from the higher order spectrum of the input and is computationally more efficient because the size of the feature vector required is typically smaller than the number of classes. The features can also be computed in parallel. Monte Carlo simulations show that the technique is capable of high classification accuracy at low signal-to-noise ratios. The present study is restricted to classification of one-dimensional inputs and features derived from the bispectrum, and focuses on the new technique. Invariants defined from the bispectrum are presented in Section II. The significance

Manuscript received February 7, 1991; revised September 28, 1991. This work was supported by the Office of Naval Research, Coastal Sciences.

The authors are with the Department of Electrical Engineering and Computer Science, Washington State University, Pullman, WA 99164-2752.

IEEE Log Number 9203353.

of the feature values in terms of the symmetry of the pattern and the procedures for feature extraction from symmetric patterns are described in Section III, while feature extraction from multiple realizations of noisy patterns is discussed in Section IV. The training and classification procedures are explained in Section V, followed by an application demonstrating the ability of the procedure to distinguish similar, but different bolts, and Monte Carlo simulations to test the classification accuracy of the method on noisy input data in Section VI.

II. Bispectral Invariants

The bispectrum $B(f_1, f_2)$ of a one-dimensional, deterministic, discrete-time signal, $x(n)$, is defined as

$$B(f_1, f_2) = X(f_1)X(f_2)X^*(f_1 + f_2) \tag{1}$$

where $X(f)$ is the discrete-time Fourier transform of $x(n)$ and f is normalized frequency. By virtue of its symmetry properties, the bispectrum of a real signal is uniquely defined by its values in the triangular region of computation, $0 \le f_2 \le f_1 \le f_1 + f_2 \le 1$, provided there is no bispectral aliasing [3].

Parameters, $P(a)$, that are translation, dc-level, amplification, and scale invariant, are defined from the bispectrum of $x(n)$ as follows:

$$P(a) = \arctan\left(\frac{I_i(a)}{I_r(a)}\right) \tag{2}$$

where

$$I(a) = I_r(a) + jI_i(a) = \int_{f_1 = 0^+}^{1/(1+a)} B(f_1, af_1)\, df_1 \tag{3}$$

for $0 < a \le 1$, and $j = \sqrt{-1}$.

Note that the bispectral values are integrated along straight lines with slope a passing through the origin in the bifrequency space, as shown in Fig. 1.

Claim: $P(a)$ are translation invariant.

Proof: Any time shift in the sequence $x(n)$ introduces a linear, frequency dependent phase shift in its Fourier transform $X(f)$, and this phase shift is cancelled in the triple product defined in (1). Thus, the bispectrum is translation invariant. Integrating the bispectrum along lines passing through the origin in bifrequency space preserves the translation invariance because the integral is translation invariant if the integrand is. Finally, the phase of the complex entity $I(a)$ must also be translation invariant because its real and imaginary parts are. Thus, $P(a)$ are translation invariant.

Claim: $P(a)$ are dc-level invariant.

Proof: A constant added to the sequence $x(n)$ changes only the discrete-time Fourier transform coefficient $X(0)$. Therefore, only those bispectral values change for which either f_1 or f_2 is zero. The definition of $P(a)$ excludes these bispectral values because the integration (see (3)) is from $f_1 = 0^+$ to $f_1 = 1/(1 + a)$ and a is strictly positive.

Claim: $P(a)$ are amplification invariant.

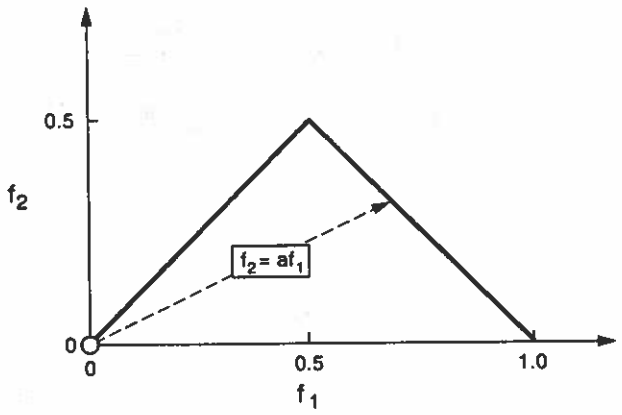

Fig. 1. The bispectrum is integrated along the dashed line and the phase is taken to yield feature $P(a)$. Frequencies f_1 and f_2 are shown normalized by one half the sampling frequency, and the triangular region is the region of computation of the bispectrum assuming no bispectral aliasing.

Proof: Multiplication of the sequence $x(n)$ by a constant affects the real and imaginary parts of $X(f)$ equally, and hence, the real and imaginary parts of the bispectrum and the integrated bispectrum $I(a)$, also equally. Therefore, $P(a)$ will remain invariant for any a.

Claim: $P(a)$ are scale invariant.

Proof: Scaling involves decimation or interpolation of the sequence $x(n)$.

Let the sequence $x(n)$ be interpolated by scale factor s (an integer greater than 1) to yield $x(n/s)$. Assume that $X(f)$ is band limited, such that $X(f) = 0$ for $|f| > 1/(2s)$. Although this assumption is not strictly true for duration-limited signals and signals of interest in pattern recognition are duration limited, it is a good assumption provided $X(f)$ is negligible for $|f| > 1/(2s)$. The discrete-time Fourier transform, $X_s(f)$, of the scaled sequence is given by $sX(sf)$. The bispectrum of the scaled signal, $B_s(f_1, f_2)$ is given by $s^3B(sf_1, sf_2)$. Let $I_s(a)$ denote the integrated bispectrum of the scaled signal. Note also that since $0 < a \le 1 < s$,

$$0 < \frac{1}{2s} < \frac{1}{2} \le \frac{1}{1+a} < 1$$

and the upper limit of the integral defining $P(a)$ can be any frequency in the interval $[1/(2s), 1/(1 + a)]$ because $X(f)$ is band limited to $1/(2s)$. Then

$$\begin{aligned} I_s(a) &= \int_{f_1 = 0^+}^{1/(1+a)} s^3 B(sf_1, asf_1)\, df_1 \\ &= \int_{f_1 = 0^+}^{1/(2s)} s^3 B(sf_1, asf_1)\, df_1 \\ &= s^2 \int_{f_1 = 0^+}^{1/2} B(f_1, af_1)\, df_1 \\ &= s^2 \int_{f_1 = 0^+}^{1/(1+a)} B(f_1, af_1)\, df_1 \\ &= s^2\, I(a). \end{aligned} \tag{4}$$

Since s is a real constant, the phase of $I_s(a)$ is the same as the phase of $I(a)$. Thus, $P(a)$ are invariant to interpolation under the band-limited assumption.

Let the sequence $x(n)$ be decimated by S (an integer greater than 1) to yield $x(Sn)$. Then the discrete-time Fourier transform of the decimated sequence is $(1/S)$ $X(f/S)$ and the bispectrum is $(1/S^3)$ $B(f_1/S, f_2/S)$. Assume again that $x(n)$ is band limited, such that $X(f) = 0$ for $|f| > 1/(2S)$. Note also that since $0 < a \leq 1 < S$,

$$0 < \frac{1}{2S} \leq \frac{1}{S(1+a)} < \frac{1}{(1+a)} < 1$$

and the upper limit of the integral defining $P(a)$ can be any frequency in the interval $[1/(2S),\ 1/(1+a)]$ because $X(f)$ is band limited to $1/(2S)$. If $I_S(a)$ denotes the integrated bispectrum of the decimated sequence, then similar to (4), it can be shown that

$$I_S(a) = \frac{1}{S^2} I(a). \tag{5}$$

Since S is a real constant, the phase of $I_S(a)$ is the same as the phase of $I(a)$. Thus, $P(a)$ are invariant to decimation under the band-limited assumption.

If the input is not strictly band limited as assumed above, the parameters $P(a)$ will not be strictly invariant for scaled inputs, and the minimal set of parameters for classification is selected taking this into consideration.

The computational procedure to calculate $P(a)$ given an N-point real sequence $x(n)$ is as follows. The sequence is discrete Fourier transformed (using an FFT routine) to yield $X(k)$. The bispectrum is calculated as

$$B(k_1, k_2) = X(k_1)X(k_2)X^*(k_1 + k_2) \tag{6}$$

for $0 \leq k_2 \leq k_1 \leq k_1 + k_2 \leq (N/2 - 1)$. The integral in (3) is approximated by a sum, yielding

$$I(a) = \sum_{k_1=1}^{\lfloor (N/2-1)/(1+a) \rfloor} B(k_1, ak_1) \tag{7}$$

for $0 < a \leq 1$. The bispectrum is interpolated for this summation by

$$B(k_1, ak_1) = pB(k_1, \lceil ak_1 \rceil) + (1 - p)\, B(k_1, \lfloor ak_1 \rfloor) \tag{8}$$

where $p = ak_1 - \lfloor ak_1 \rfloor$, $\lfloor x \rfloor$ represents the largest integer contained in x, and $\lceil x \rceil$ represents the smallest integer containing x. The invariant parameters $P(a)$ are the principal component of the phase of $I(a)$, $-\pi < P(a) \leq +\pi$.

III. Features from Symmetric and Asymmetric Patterns

It is well known that the phase of the bispectrum is related to the shape of the signal, and thus some general observations can be made about $P(a)$ for signals according to their symmetry. Consider a real signal $x(n)$ that has nonzero values only over a finite region of support, say $N_1 \leq n \leq N_2$. Since the parameters $P(a)$ are dc-level invariant, a pattern over a finite support embedded in a constant background is equivalent to such a $x(n)$.

A. P(a) for Even-Symmetric Patterns

An even-symmetric sequence has a discrete-time Fourier transform whose phase is linear with frequency. This phase is cancelled in the triple product defined in (1). Therefore, the bispectrum is real. The integrated bispectrum is also real (positive or negative), and $P(a) = 0$ if $I(a)$ is positive, or $P(a) = \pi$ if $I(a)$ is negative, for $0 < a \leq 1$.

Note that if the even-symmetric sequence, $x(n)$, is negated, the negative sequence will have those parameters $P(a)$ that were originally equal to zero take on value π, and those parameters $P(a)$ that were originally equal to π take on value zero.

B. P(a) for Odd-Symmetric Patterns

An odd symmetric sequence has a discrete-time Fourier transform whose phase is linear with frequency plus a constant phase of $\pi/2$. Therefore, the bispectrum is imaginary. The integrated bispectrum is also imaginary, and $P(a) = \pi/2$ if $I(a)$ is positive, or $P(a) = \pi/2$ if $I(a)$ is negative, for $0 < a \leq 1$.

Note that if the odd-symmetric sequence, $x(n)$, is negated, then the parameters $P(a)$ will also be negated.

C. P(a) as Features for Asymmetric Patterns

Any arbitrary, real sequence $x(n)$ that has nonzero values only over a finite region of support, say $N_1 \leq n \leq N_2$, can be expressed as

$$x(n) = Ax_e(n) + Bx_o(n) \tag{9}$$

where $x_e(n)$ is even-symmetric about $(N_1 + N_2)/2$, the center of the region of support, and $x_o(n)$ is odd-symmetric about $(N_1 + N_2)/2$, and A, B are real constants.

The phase of the Fourier transform of an asymmetric sequence will be a nonlinear function of frequency. This nonlinearity is isolated by the parameters $P(a)$, and thus $P(a)$ can be used as elements of a feature vector to classify asymmetric sequences.

If an asymmetric sequence is flipped about its center of support, the parameters $P(a)$ are negated because the odd component of the sequence is negated.

D. Feature Extraction from a Symmetric Pattern

For two classes of patterns that are both even symmetric or both odd symmetric, the parameters $P(a)$ defined above are the same for the two classes, and thus insufficient to discriminate between them. For example, a symmetric rectangular pulse and a symmetric triangular pulse are both linear phase and have $P(a) = 0$ for all $0 < a \leq 1$. In such a case, the phase of the Fourier transform does not contain information to distinguish the shapes. On the other hand, if the phases of the two dis-

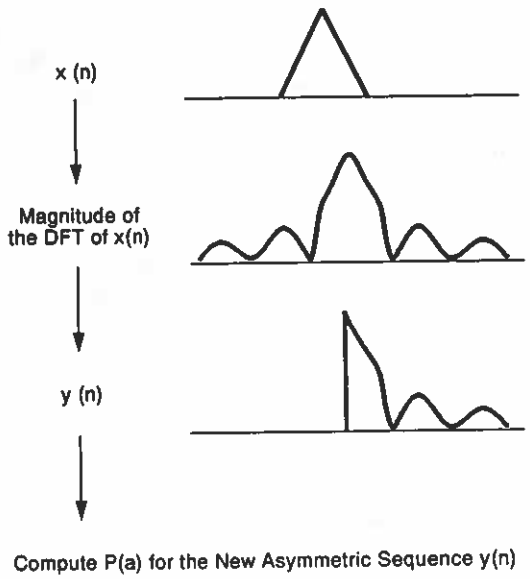

Fig. 2. The procedure to extract features $P(a)$ from a symmetric pattern $x(n)$.

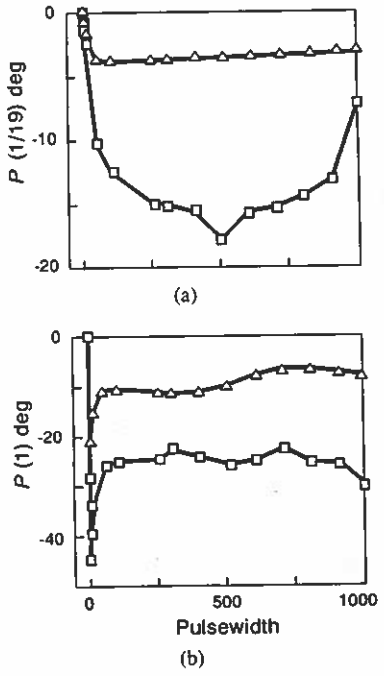

Fig. 3. Parameters $P(1/19)$ and $P(1)$ as a function of the width of the input pulse. Triangles and squares are the values for the triangular and rectangular pulse patterns, respectively. These parameters have been computed by the procedure shown in Fig. 2 for feature extraction from symmetric patterns. (a) $P(1/19)$, (b) $P(1)$.

similar sequences are identical, the Fourier magnitudes must differ. In this case, a new sequence, $y(n)$ is formed by discarding the phases and zero padding the magnitude of the Fourier transform, $|X(k)|$, of $x(n)$ for positive frequencies only. Note that by including only the right half of the symmetric Fourier transform magnitude sequence, an asymmetric sequence is obtained. The parameters $P(a)$ computed from $y(n)$ satisfy the same invariance as those computed from $x(n)$. Parameters $P(a)$ may now be computed for the $y(n)$ and used as features to discriminate between the original sequences. This procedure is illustrated in Fig. 2. Consider the case where the inputs are rectangular or triangular pulses of different widths, zero padded to 1024-point long sequences. The pulses have arbitrary amplitudes and may be translated in time or level shifted. Parameters $P(1/19)$ and $P(1)$ computed from the asymmetric sequences composed of positive frequency halves of the magnitudes of the respective Fourier coefficients are shown as a function of the width of the pulse in Figs. 3(a) and (b), respectively. Note that either parameter is sufficient to distinguish rectangular from triangular pulses over a large range of pulsewidths, and that these parameters are fairly constant in that range. When the width tends to zero, both classes of pulse tend toward a unit sample and the parameters approach zero degrees.

IV. Features from Patterns in Noise

The expected value of the bispectrum for Gaussian noise is zero and therefore the effect of noise can be reduced by averaging [2], [5], [37] the triple products of Fourier coefficients in (6) over many realizations. $P(a)$ may then be computed as the phase of this averaged integrated bispectrum. Even for the case of only one realization of a noisy pattern, the averaging that occurs by integrating the bispectrum over the many values along the line with slope a in bifrequency space before calculating the phase, $P(a)$, results in noise rejection. Examples of classification of noisy patterns are presented below.

V. Training and Classification

The feature extraction algorithm proposed in this study can be combined with any standard parametric or nonparametric classifier [16], [38]. The performance of the classifier will depend on the probability density functions of the features in feature space. The dimensionality of the feature vector can also be reduced by classical techniques such as principal component analysis [39]. If the features form isolated, compact clusters in feature space for noise-free input, the probability density functions will tend toward multivariate Gaussian as the noise power increases. Each class is then adequately described by the mean and standard deviation of the feature vector, and simpler training and classification procedures are applicable. Given below are a training procedure and a variation of the minimum distance classifier [16], [38] which work under the assumption of a Gaussian probability density. The choice of this classifier is motivated by the application to low SNR inputs. For high SNR inputs when discriminating between very similar shapes is of prime importance, and the probability density functions are unknown, other classifiers [16], [38] should perform better. The tests on noisy data, however, show that even the simple classifier used here yields high classification accuracies.

During the training phase of this classifier, parameters $P(a)$ are computed at some integer number of values of a for representative inputs from each class under consideration, at different scales. These parameters should be in-

variant within the same class under the assumptions stated in Section II. If the shape varies within a given class, the input is not strictly band limited, or the input is noisy, there will be a nonzero intraclass variance. The *intraclass mean* and *intraclass standard deviation* of $P(a)$ are computed for each class and each parameter a over the entire training data set. The *interclass separation* between two classes for a given parameter is defined as the mean-square difference between the values of $P(a)$ for the two classes over the entire training set divided by the sum of the two intraclass standard deviations. A set of parameters a to form the feature vector, $P(a)$ for the chosen values of a, is now selected as follows.

1) Choose the parameter a which yields the maximum separation between classes over all the pairs of classes and all the parameters under consideration.

2) Choose an acceptable level of separation between the maximum and minimum separations (say, midway between them), as a threshold.

3) Eliminate from further consideration those pairs of classes that have separations equal to or above this threshold.

4) If all possible pairs of classes are eliminated, the procedure is successfully completed, otherwise to go to step 1 to select an additional parameter.

Feature vectors to represent each class, i.e., model features, are formed by using the mean values of the selected parameters for that class. Although many schemes exist to select a minimal feature vector, the procedure described above is fast and worked very well for the Monte Carlo simulations discussed in Section VI.

Given an input pattern, the data feature vector (using selected parameters) is computed for the input data and compared to the model feature vectors representing each class. A minimum distance classifier is used to ascribe the input to that class whose feature vector is "closest" to that of the pattern. The distance between an element, $P(a)$ for a particular value of a, of the data feature vector and the corresponding element of a model feature vector representing a particular class is defined as the Euclidean distance between them divided by the standard deviation of the $P(a)$ for that particular class. The distance between the two feature vectors is defined as the sum of the squares of the distances between their elements. This minimum distance classifier using a statistical distance measure is also fast and yields good results, as seen in Section VI.

Although the minimum distance classifier is a linear classifier, it is possible to obtain piecewise approximations to nonlinear discriminant functions by representing each class by a set of model feature vectors instead of a single vector. An enhanced version of the training procedure described above would take this into account by dividing each class into subclasses, with each subclass representing a range of variation of the scale factor. A minimal subset of the feature vectors for each subclass is retained as a model feature vector set for the class. The procedure for feature extraction proposed here can be combined with many other classifiers [16], including a neural net classifier [27]–[29].

VI. Application

The technique described here can classify objects from one-dimensional profiles. These profiles can be obtained using a sonar or laser rangefinder which scans across the object, or an imaging device. To demonstrate the feasibility of this application, profiles of two types of bolts were selected. They may be left or right oriented, accounting for four different patterns, as shown in Fig. 4. Test sequences consisting of 1024 points were used. Fig. 5 shows a comparison of the inputs for scale factors 0.5, 1.0, and 2.0. Parameters $P(a)$ for these patterns were computed for $a = 1/19, 2/19, \cdots, 1$. Fig. 6 shows the values of a feature vector consisting of $\{P(a), a = 1/19$ and $a = 1\}$ for bolts 1 and 2 with left and right orientations, for scale variations between 0.5 and 2.0. As shown in Fig. 6, given $P(1/19)$ and $P(1)$, the two similar looking bolts clearly can be distinguished.

For noisy realizations, this particular feature vector may not be able to provide good classification accuracy. However, the training algorithm given above takes the interclass separations into account in selecting the feature vector. The classification accuracy of the method for noisy input data was tested as follows.

A. Test 1 (Invariance)

The test was performed to test the extent of invariance of the features to amplification, shift, and scaling (dc-level invariance is trivially satisfied and need not be tested). The input consisted of rectangular and triangular pulses, zero padded to form 1024-point sequences. The amplitude of each pulse was uniform random in [1, 2), the pulsewidth was uniform random in [64, 704), and the shift was uniform random in [1, 1016–pulsewidth). Uncorrelated Gaussian noise of variance 0.1 was added to each input. The training set consisted of 32 realizations from each class. The feature extraction procedure shown in Fig. 2 was employed. A feature vector composed of the single feature, $P(9/19)$, was selected by the training algorithm. For the triangular pulses, $P(9/19)$ had a mean value of $-11.0°$ and a standard deviation of $1.4°$, over the training data set. For the rectangular pulses, the mean and standard deviation of $P(9/19)$ were $-21.0°$ and $0.6°$, respectively. The classifier was tested with 128 realizations from each class, and the classification accuracy was 100%, verifying the invariance properties of the feature vectors.

B. Test 2 (No Ensemble Averaging)

The classifier was trained using 32 noisy realizations from each of the four classes of bolts shown in Fig. 4. The noise was additive Gaussian, uncorrelated with the pattern, and the signal-to-noise ratio (SNR) was 10 dB. The acceptable level of separation between classes was

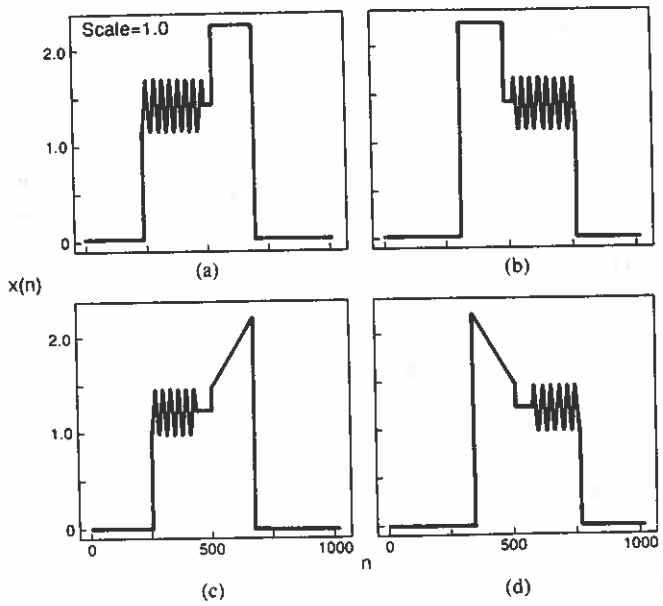

Fig. 4. The four classes of patterns. (a), (b) Bolt 1 and (c), (d) Bolt 2.

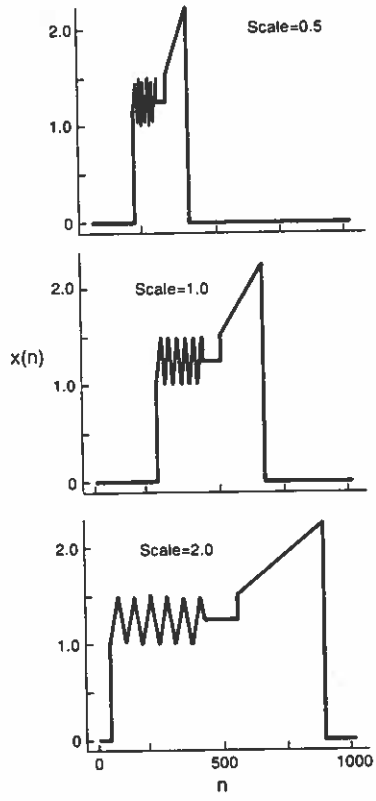

Fig. 5. Bolt 2 (pattern (c) in Fig. 4) shown for scale factors 0.5, 1.0, and 2.0.

set to be one half the sum of the maximum and minimum separations. The feature vector selected was composed of parameters $P(14/19)$ and $P(1)$. Table I shows the means and standard deviations of these parameters for each class, over the 32 realizations in the training set. The classifier was then tested with 132 realizations (input test data) from each class for SNR equal to 10, 3, 0, and -3 dB. The classification accuracy as a function of SNR is shown in

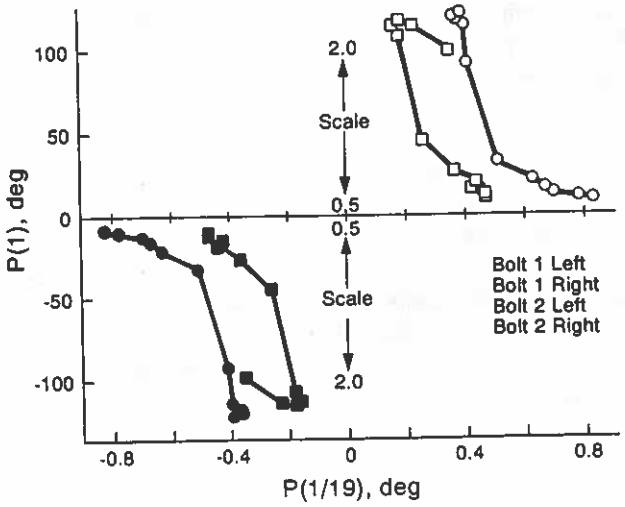

Fig. 6. A feature vector comprising $P(1/19)$ and $P(1)$ traced as the scale factor is varied from 0.5 to 2.0 for the four patterns shown in Fig. 4.

TABLE I
MEAN VALUES AND STANDARD DEVIATIONS, IN DEGREES, FOR THE FEATURE ELEMENTS, $P(14/19)$ AND $P(1)$, SELECTED TO FORM THE FEATURE VECTOR IN TEST 2. THE FOUR CLASSES OF PATTERN, (a), (b), (c), AND (d), CORRESPOND TO THE BOLTS SHOWN IN FIG. 4. THE STANDARD DEVIATIONS ARE THE NUMBERS SHOWN BELOW THE MEAN VALUES IN EACH BOX

Feature Element	Class (a)	(b)	(c)	(d)
$P(14/19)$	25.2 ±1.2	−25.1 ±1.1	21.1 ±1.1	−21.2 ±1.2
$P(1)$	45.0 ±3.1	−45.1 ±2.5	32.7 ±2.3	−32.7 ±2.4

Fig. 7. Note that the classification accuracy is high even without any ensemble averaging in the feature extraction phase because some averaging is obtained by the integration over bifrequencies implicit in the calculation of $I(a)$ (7).

C. Test 3 (Ensemble Averaging)

For this test the input data (both training and testing) was available in ensembles of 16 realizations each. The classifier was trained using 32 noisy (10-dB SNR) ensembles from each class. The noise was additive Gaussian, uncorrelated with the pattern. Features were computed after averaging the bispectra of the 16 realizations in each ensemble. The acceptable level of separation between classes was again set to be one half the sum of the maximum and minimum separations. The feature vector selected was composed of $P(13/19)$ and $P(1)$. Table II shows the means and standard deviations of these parameters for each class, over the training data set. The classifier was then tested with 64 ensembles from each class for SNR of 10, 3, 0, and -3 dB. Fig. 8 shows the classification accuracies obtained in each case. Note that the classification accuracy for bispectra computed from an

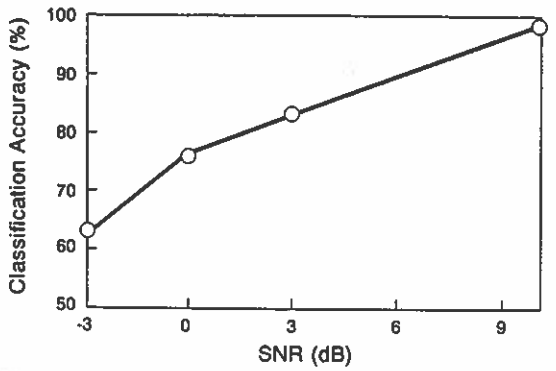

Fig. 7. Classification accuracy versus the signal-to-noise ratio of the test patterns for test 2. There was no ensemble averaging in the feature extraction phase for this test. The training set had a 10-dB SNR.

TABLE II
MEAN VALUES AND STANDARD DEVIATIONS, IN DEGREES, FOR THE FEATURE ELEMENTS, $P(13/19)$ AND $P(1)$, SELECTED TO FORM THE FEATURE VECTOR IN TEST 3. THE FOUR CLASSES OF PATTERN, (a), (b), (c), AND (d), CORRESPOND TO THE BOLTS SHOWN IN FIG. 4. THE STANDARD DEVIATIONS ARE THE NUMBERS SHOWN BELOW THE MEAN VALUES IN EACH BOX. THE BISPECTRUM WAS AVERAGED FOR 16 REALIZATIONS BEFORE COMPUTING THE FEATURE ELEMENTS, ACCOUNTING FOR THE LOWER STANDARD DEVIATIONS

Feature Element	Class (a)	(b)	(c)	(d)
$P(13/19)$	21.8 ±0.3	−21.8 ±0.3	19.0 ±0.2	−18.9 ±0.2
$P(1)$	44.9 ±0.9	−44.9 ±0.7	32.6 ±0.6	−32.5 ±0.6

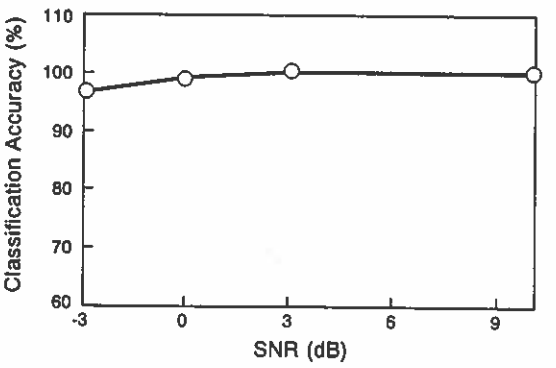

Fig. 8. Classification accuracy versus the signal-to-noise ratio of the test patterns for test 3. Bispectra from 16 realizations were averaged to compute the feature elements for this test. The training set had a 10-dB SNR.

ensemble of realizations is significantly higher than the accuracy obtained when only one realization is available (compare Figs. 7 and 8).

VII. CONCLUSION

Phases of integrals of the bispectrum are shown to be translation, dc-level, amplification, and scale invariant, and can be used to classify patterns. A minimal set of these invariants can be selected as a feature vector, allowing similar patterns to be distinguished. Two similar shaped, one-dimensional bolts are readily distinguished even for inputs with low signal-to-noise ratios because the higher order spectral approach to pattern classification has high immunity to additive Gaussian noise. A 1024-point FFT can be performed rapidly, and formation of the triple products of Fourier coefficients and the summations required to determine the features can be implemented in parallel. Thus, the approach to distinguishing patterns presented here is fast. Extensions to two-dimensional objects will be presented in another paper.

REFERENCES

[1] K. Hasselmann, W. H. Munk, and G. J. F. MacDonald, "Bispectra of ocean waves," in *Time Series Analysis*, M. Rosenblatt, Ed. New York: Wiley, 1963, pp. 125-139.
[2] D. R. Brillinger and M. Rosenblatt, "Asymptotic theory of estimates of *k*th order spectra," in *Spectral Analysis of Time Series*, B. Harris, Ed. New York: Wiley, 1967, pp. 153-188.
[3] D. R. Brillinger and M. Rosenblatt, "Computation and interpretation of *k*th order spectra," in *Spectral Analysis of Time Series*, B. Harris, Ed. New York: Wiley, 1967, pp. 189-232.
[4] Y. C. Kim and E. J. Powers, "Digital bispectral analysis and its applications to nonlinear wave interactions," *IEEE Trans. Plasma Sci.*, vol. 7, pp. 120-131, 1979.
[5] C. L. Nikias and M. R. Raghuveer, "Bispectrum estimation: A digital signal processing framework," *Proc. IEEE*, vol. 75, pp. 869-889, 1987.
[6] H. Bartelt and B. Wirnitzer, "Shift-invariant imaging of photon-limited data using bispectral analysis," *Opt. Commun.*, vol. 53, pp. 13-16, 1985.
[7] M. R. Raghuveer and S. A. Dianat, "Detection of nonlinear phase coupling in multi-dimensional stochastic processes," in *Proc. Int. Conf. Adv. Contr. Commun.*, Oct. 1988, pp. 729-732.
[8] A. Swami and G. B. Giannakis, "ARMA modeling and phase reconstruction of multidimensional non-Gaussian processes using cumulants," in *Proc. ICASSP-88*, New York, NY, Apr. 1988, pp. 729-732.
[9] G. B. Giannakis, "Cumulants: A powerful tool in signal processing," *Proc. IEEE*, pp. 1333-1334, Sept. 1987.
[10] H. Bartelt, A. W. Lohmann, and B. Wirnitzer, "Phase and amplitude recovery from bispectra," *Appl. Opt.*, pp. 3121-3129, Sept. 1984.
[11] T. Matsuoka and T. J. Ullrych, "Phase estimation using the bispectrum," *Proc. IEEE*, pp. 1403-1411, Oct. 1984.
[12] V. Chandran and S. Elgar, "Bispectral analysis of two-dimensional random processes," *IEEE Trans. Acoust., Speech, Signal Processing*, pp. 2181-2186, Dec. 1990.
[13] A. V. Oppenheim and J. S. Lim, "The importance of phase in signals," *Proc. IEEE*, pp. 529-541, May 1981.
[14] W. Eric and L. Grimson, *Object Recognition by Computer: The Role of Geometric Constraints*. Cambridge, MA: M.I.T. Press, 1990.
[15] K. S. Fu, *Syntactic Pattern Recognition and Applications*. Englewood Cliffs, NJ: Prentice-Hall, 1982.
[16] K. Fukunaga, *Introduction to Statistical Pattern Recognition*. New York: Academic, 1972.
[17] D. H. Ballard, "Generalizing the Hough transform to detect arbitrary patterns," *Patt. Recog.*, vol. 13, pp. 111-122, 1981.
[18] L. S. Davis, "Shape matching using relaxation techniques," *IEEE Trans. Patt. Anal. Machine Intell.*, pp. 60-72, Jan. 1979.
[19] E. Persoon and K. S. Fu, "Shape discrimination using Fourier descriptors," *IEEE Trans. Syst., Man, Cybern.*, pp. 388-397, Mar. 1977.
[20] T. P. Wallace and P. A. Wintz, "An efficient three-dimensional aircraft recognition algorithm using normalized Fourier descriptors," *Comput. Graph. Image Processing*, vol. 13, pp. 99-126, 1980.
[21] C. C. Lin and R. Chellappa, "Classification of partial 2-D shapes using Fourier descriptors," *IEEE Trans. Patt. Anal. Machine Intell.*, pp. 686-689, Sept. 1987.
[22] M. K. Hu, "Visual pattern recognition by moment invariants," *IRE Trans. Inform. Theory*, pp. 179-187, Feb. 1962.
[23] A. Khotanzad and Y. H. Hong, "Rotation and scale invariant features

for texture classification," in *Proc. Robotics and Automation, IASTED* (Santa Barbara, CA), May 1987, pp. 16–17.
[24] Y. S. Abu Mostafa and D. Psaltis, "Recognitive aspects of moment invariants," *IEEE Trans. Patt. Anal. Machine Intell.*, pp. 698–706, June 1984.
[25] B. Bamieh and R. J. P. De Figueiredo, "A general moment invariants-/attributed-graph method for three-dimensional object recognition from a single image," *IEEE J. Robot. Automation*, pp. 31–41, Feb. 1986.
[26] T. Kohonen, "Learning vector quantization for pattern recognition," Tech. Rep. TKK-F-A601, Helsinki Univ. Technology, Helsinki, Finland, Nov. 1986.
[27] F. Rosenblatt, *Principles of Neurodynamics: Perceptrons and the Theory of Brain Mechanisms*. Washington, DC: Spartan, 1961.
[28] J. J. Hopfield, "Neural networks and physical systems with emergent collective computational abilities," *Proc. Nat. Acad. Sci.*, vol. 79, pp. 2554–2558, 1982.
[29] R. P. Lippmann, "An introduction to computing with neural nets," *IEEE ASSP Mag.*, pp. 4–22, Apr. 1987.
[30] T. Kohonen, G. Barna, and R. Chrisley, "Statistical pattern recognition with neural networks: Benchmarking studies," in *IEEE Proc. ICNN*, vol. 1, July 1988, pp. 61–68.
[31] D. Casasent and D. Psaltis, "Position, rotation, and scale invariant optical correlation," *Appl. Opt.*, vol. 15, pp. 1795–1799, Oct. 1976.
[32] L. Capodiferro, R. Gusani, G. Jacoviti, and M. Vascotto, "A correlation based technique for shift, scale, and rotation independent object identification," in *Proc. Int. Conf. Acoust., Speech, Signal Processing* (Dallas, TX), 1987, pp. 221–224.
[33] B. M. Sadler, "Shift and rotation invariant object reconstruction using the bispectrum," in *Proc. Workshop Higher Order Spectral Analysis*, June 1989, pp. 106–111.
[34] M. K. Tsatsanis and G. B. Giannakis, "Object detection and classification using matched filtering and higher order statistics," in *Proc. 6th Workshop Multidimensional Signal Processing* (Pacific Grove, CA), Sept. 1989, pp. 32–33.
[35] M. K. Tsatsanis and G. B. Giannakis, "Translation, rotation and scaling invariant object and texture classification using polyspectra," *Proc. SPIE Int. Soc. Opt. Eng.*, vol. 1348, pp. 103–115, July 1990.
[36] G. B. Giannakis and M. K. Tsatsanis, "Signal detection using matched filtering and higher order statistics," *IEEE Trans. Acoust., Speech, Signal Processing*, vol. 38, pp. 1284–1296, July 1990.
[37] M. J. Hinich, "Detecting a transient signal by bispectral analysis," *IEEE Trans. Acoust., Speech, Signal Processing*, vol. 38, pp. 1277–1283, July 1990.
[38] R. O. Duda and P. E. Hart, *Pattern Classification and Scene Analysis*. New York: Wiley Interscience, 1973.
[39] C. R. Rao, "The use and interpretation of principal component analysis," *Sankhya Ind. J. Stat. A*, vol. 26, pp. 329–358, 1964.

Vinod Chandran (S'85–M'90) received the B.Tech degree in electrical engineering from the Indian Institute of Technology, Madras, India, in 1982, the M.S.E.E. degree from Texas Tech University, Lubbock, in 1985, and the Ph.D. degree in electrical and computer engineering and the M.S.C.S. degree, both from Washington State University, Pullman, in 1990 and 1991, respectively.

Since August 1990 he has been a Postdoctoral Teaching Associate in the School of Electrical Engineering and Computer Science, Washington State University. His research interests include pattern recognition, higher order spectral and cumulant based techniques, and speech analysis.

Dr. Chandran is a member of the Optical Society of America, Tau Beta Pi, and Phi Kappa Phi, and an associate member of Sigma Xi.

Stephen L. Elgar (A'87) received the bachelor's degree in mathematics and civil engineering from the University of Idaho, Moscow, in 1980, and the master's and Ph.D. degrees in oceanography from the Scripps Institution of Oceanography, University of California, San Diego, in 1981 and 1985, respectively.

In 1986 he joined the Department of Electrical Engineering at Washington State University, Pullman. His current research interests involve the study of nonlinear waves, in particular, ocean surface gravity waves and signal processing techniques necessary for analyzing ocean field measurements. In addition, his interests have included studies of irrigation canals, chaos, flows behind vibrating cylinders, image processing, and global temperatures during the last 2–3 million years.

Dr. Elgar is a member of the American Geophysical Union, the American Physical Society, and the American Meteorological Society. He is an Associate Editor for the IEEE TRANSACTIONS ON SIGNAL PROCESSING.